

Laboratory Experiment for End Bearing Capacity of Pile with Fragile Root Solidifying Part

Hideyo Sato

Department of Architecture & Life Design, Nihon University Junior College, Funabashi, Chiba, Japan

Katsuhiro Kanuka

Kanuka Design Co., Ltd, Nishi-ku, Yokohama, Kanagawa, Japan

Sena Miyazaki

Kanuka Design Co., Ltd, Nishi-ku, Yokohama, Kanagawa, Japan

Toru Osakabe

Division of Architecture & Civil Engineering, Ashikaga Institute of Technology, Ashikaga, Tochigi, Japan

Shozo Wada

Division of Architecture & Civil Engineering, Ashikaga Institute of Technology, Ashikaga, Tochigi, Japan

ABSTRACT

The cement milk pile construction method is classified into the prebored pile construction method, and the pile tip is solidified with the cement paste. In this method, precast concrete pile or steel pipe pile is used, and its pile end has a circular opening. The objective of this study is to develop an effective pile end shape for a small-diameter steel pipe pile, which can work even if the stiffness of the cement milk around the pile tip would be insufficient. Laboratory experiments for static axial compressive load tests of single piles covered with un-hardened clay around the pile end were performed. The end bearing capacity, that is, the resistance of the pile tip when the pile tip displacement reaches to 10% of the pile diameter, of the open end pile was less than 20% of the standard pile. Also, the end disk plate appended to the pile tip worked effectively. An observation test to investigate the deformation process of the root part was also performed. When the vertical displacement progressed, a swelling was observed at the bottom and the sides of the root part, and finally, punching destruction happened.

KEY WORDS: Cement milk pile construction method; end bearing capacity; laboratory experiment.

INTRODUCTION

Recently, the application number of the cement milk pile construction method is increasing in urban areas of Japan because of less construction noise and vibration. Furthermore, this method using small-diameter steel pipe piles can be applied to small buildings and retaining walls. With this method, it is necessary to build a homogeneous and a strong root solidifying part in the pile tip zone. If the pile end is fixed in a hard sandy soil or a gravel layer with good quality cement milk, it will show enough vertical bearing capacity. However, in a soft or a medium cohesive soil layer, the vertical resistances can be reduced by deformation or destruction of the root part. Since small-diameter steel pipe piles are often fixed to such

cohesive layers, the pile end resistance may be insufficient.

Some destruction patterns in the root solidifying part have been observed in previous research. Ueno and Kurachi (1993) reported compressive destruction and punching destruction as typical patterns. Kiya and Kato (2007) pointed out a thin root solidifying part can be the cause of the punching destruction, while a thick case can cause cracking and breakage.

On the other hand, Goto and Katsumi (1967) stated that the soil blockade of the pile tip does not take place in the case of a large diameter open end pile. In addition, Katsumi and Kitani (1982) indicated that the end bearing capacity of an open end pile and a closed end pile cannot be evaluated with same way, because the capacities depend on the sectional areas of the pile ends. Miyazaki and Sato (2014 and 2015) reported that the end disk plate attached to the pile tip is effective to exhibit good performance of the end bearing capacity for a small-diameter steel pipe pile.

The objective of this study is to make clear the characteristics of the end bearing capacity of small-diameter steel pipe pile of which root solidifying part is weak. The authors performed small sized model tests of static axial compressive loading for single piles. Air dry silica sand was used and a model pile was set up simulating actual stress condition of the prebored pile construction method in the pile end area. We discuss the end shape of the pile and the root solidifying part to obtain sufficient resistance of the pile end.

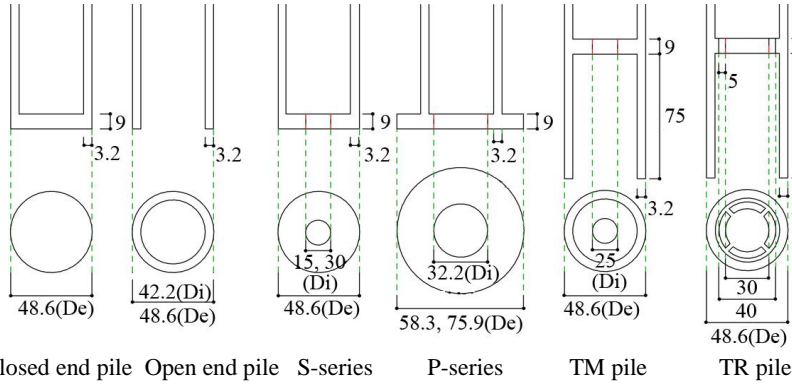
VERTICAL LOADING TEST

Test Piles and Test Series

A steel pipe, 48.6 mm in diameter (D) and 3.2 mm in thickness (t), was used as test pile. The length of the pile is 600 mm and the length of embedment (H) is 243 mm ($5D$). To eliminate frictional resistance, the pile surface was coated with Teflon. The pile ends were covered with un-hardened clay in order to imitate root solidifying parts with insufficient stiffness.

Fig. 1 and table 1 show the test pile shapes and details. A steel pipe with a steel disk (48.6 mm in diameter) attached at the tip is used as a

closed end pile (SP). In this paper, the SP is not covered with clay and is treated as the standard pile. CPT-20 and CPT-50 are performed to investigate the influence of the root thickness (R_t) below the pile tip. A test pile without modified tip and covered with clay is used as an open end pile (OPT). A test series of S is carried out to discuss the pile-end opening. At the pile tips of the S-series, holed disks with an external diameter (D_e) of 48.6 mm and an inner opening diameters (D_i) of 15, 25 and 30 mm are attached. Furthermore, a series of P is executed to investigate the effect of the pile-end area. Holed disks with an opening diameter (D_i) of 32.2 mm and external diameters (D_e) of 58.3, 67.6 and 75.9 mm are fixed to the pile tips. A series of T is carried out to evaluate the blockage effect. Disks with different shaped openings are installed to the inner part of the pile tips. The TM-25 has a circular opening with a diameter of 25 mm, and TR-5 has 4 oval openings with an area equal to TM-25.



Model Ground Preparation

A steel circular test tank with a diameter of 1,000 mm and a depth of 1,000mm is used. No. 5 silica sand in dry condition is used for the model ground. The test ground is prepared by the air-pluviation technique with double nets for dispersion. The characteristics of the model ground are shown in table 2.

In order to produce pile tip peripheral ground conditions approximate to the prebored pile construction method, model ground preparation and setting up of the test pile is executed as follows.

1. The model ground is built up to the bottom of the test pile (including the root part).
2. The test pile covered by clay is placed in the center of the tank.
3. The test tank is filled to the rim.

Converted N-values, calculated by each displacement of one drive in

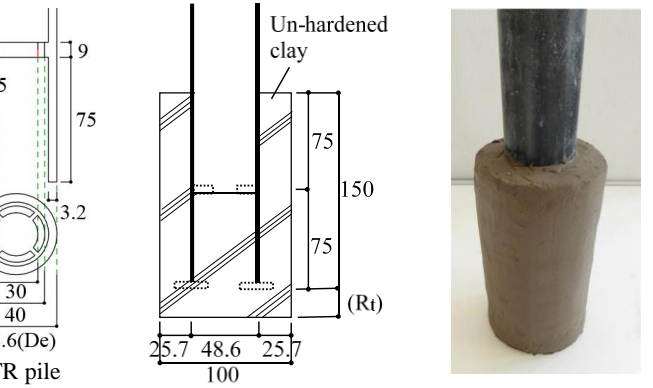


Table 1 Test pile factors

Series	Symbol	Opening area ratio of pile end (r)	Opening diameter of pile end D_o (mm)	External diameter of pile end D_e (mm)	Thickness of bottom R_t (mm)
Closed end pile	SP(Standard)	0.00	-	48.6	-
	CPT-20				20
	CPT-50				50
Open end pile	OPT	0.75	42.2	48.6	20
S-series	S-15	0.10	15.0	48.6	20
	S-30	0.38	30.0	48.6	20
P-series	P-58	0.31	32.2	58.3	20
	P-75	0.18	32.2	75.9	20
T-series	TM-25	0.26	25.0	48.6	20
	TR-5	0.27	-	48.6	20

Table 2 Model ground characteristics

Sand	Silica sand (No.5)
Method	Air-pluviation
Density (ρ)	1760 kg/m ³
Void ratio (e)	0.512
Relative density (D_r)	87.50 %
Internal friction angle (ϕ)	45°

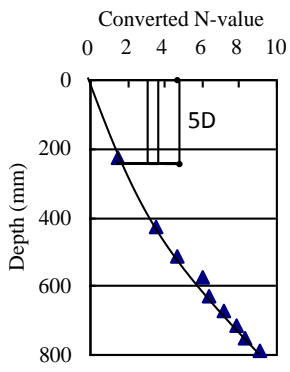


Fig. 2 Distribution of N-values

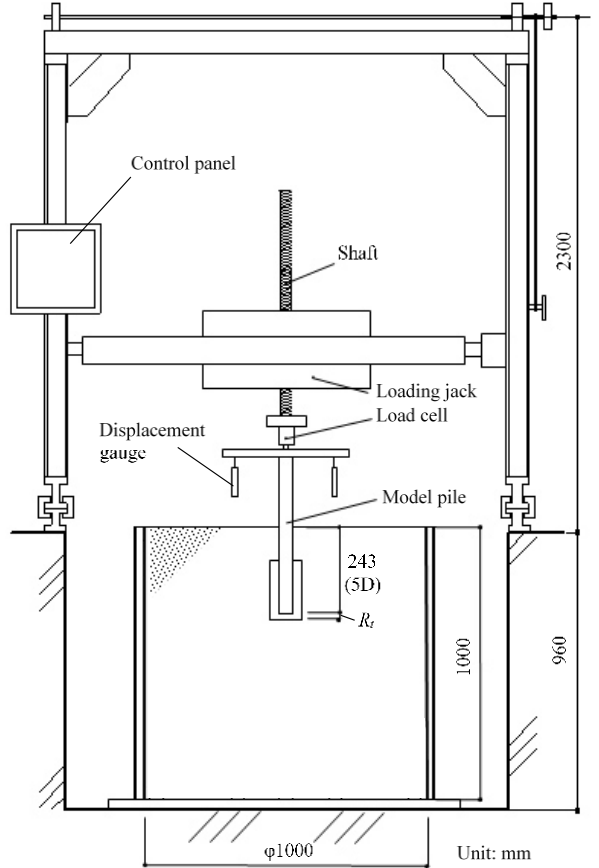


Fig. 3 Experimental apparatus

the SPT (Standard Penetration Test), are shown in fig. 2. From fig. 2, the average N -value (\bar{N}) of the pile end ($H = 243$ mm) is estimated $N = 2$.

Loading and Measurement Method

For axial loading test, a displacement controlling type loading device is used (see fig. 3), and the loading speed is 1 mm/min. The pile head load and displacement are measured in intervals of 3 seconds by load cell and two displacement gages.

In this laboratory experiment, the resistance and the displacement of the pile end are almost equal to the values of the pile head, because the pile length is relatively short and frictional resistance of the pile surface is very small. Accordingly, in this paper, the pile head load and pile head displacement are estimated as the pile end resistance and the pile end displacement, respectively.

RESULTS OF LABORATORY EXPERIMENT

Fig. 4 shows the test results of the close end piles and the open end pile. Figs. 5 to 6 show the results of the S-series, P-series and T-series, the relationships between the pile end resistance (R) and dimensionless displacement (δ/D , δ : displacement of pile end, D : diameter of pile body). Furthermore, the results of the closed end pile without fragile root (SP: standard pile) is added to the figures.

In Japan, the end bearing capacity of a single pile is calculated by Eq. 1 which is generally used in the design of pile foundation.

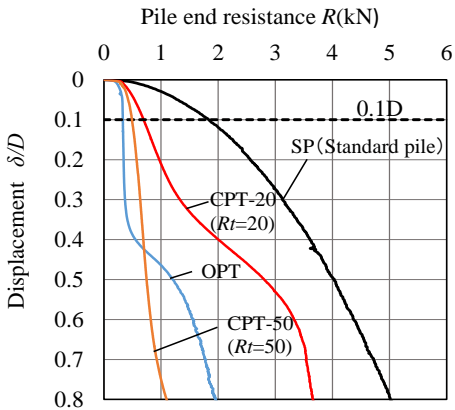


Fig. 4 Relationship between displacement and pile end resistance (open end pile, closed end pile)

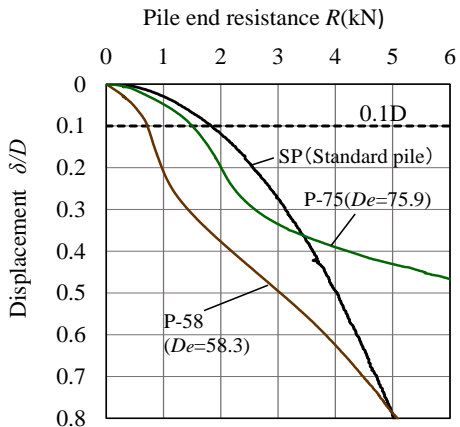


Fig. 6 Relationship between displacement and pile end resistance (P-series)

$$R_p = \alpha \cdot \bar{N} \cdot A_p \quad (1)$$

Where, R_p is the end bearing capacity, α is the bearing capacity factor, \bar{N} is the average of the N -value at pile end and A_p is the area of the pile tip. The end bearing capacity is given when the pile-end displacement reaches 10 % of the diameter. The standard value of the bearing capacity factor α for the prebored construction method is $\alpha=200$. In addition, the standard value of α for the driving construction method is $\alpha=300$.

Closed End Pile and Open End Pile

Although the model piles with fragile root part (CPT-20,CPT-50 and OPT) show smaller pile end resistances (R) than that of the standard pile (SP) in the early stage, the R values increase where δ/D exceeded around 0.3. However, R values of CPT-20, CPT-50 and OPT are smaller than the values of SP even when the δ/D reaches 0.8. The cause of the above phenomenon is because the energy of the vertical load was consumed only for deformation and destruction of the clay at the root part, but the energy is not transmitted to the support layer. As for this phenomenon, the open end pile (OPT) gives the impression stronger than the closed end pile. Moreover, this tendency of CPT-50 which has a thick root is stronger than CPT-20. The magnitude order of the end resistance (R_p), when the displacement reaches $0.1D$, is CPT-20 > CPT-50 > OPT, and the percentages of those resistances against the values of the standard pile are 38%, 27% and 18%, respectively.

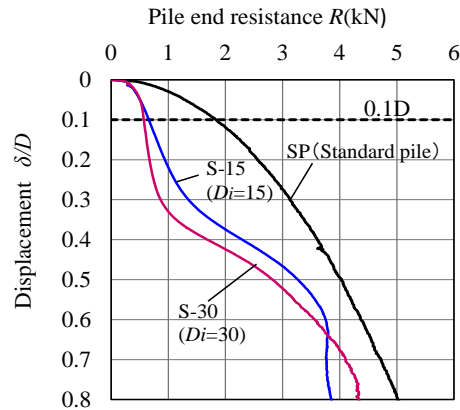


Fig. 5 Relationship between displacement and pile end resistance (S-series)

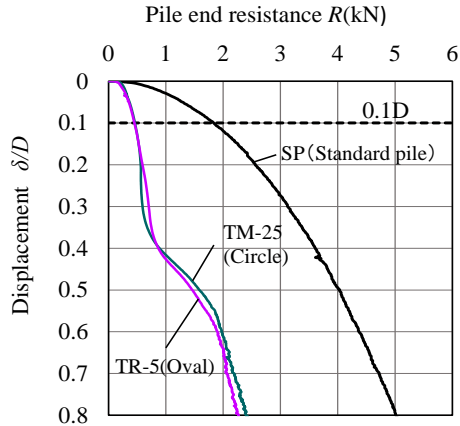


Fig. 7 Relationship between displacement and pile end resistance (T-series)

S-series, P-series and T-series

In the S-series, the larger the opening diameter of D_i at the pile end, the smaller the pile end resistance value. However, the end bearing capacities (R_p) of S-15 and S-30 are almost the same. Those values are 36% of SP's in S-15, and 31% in S-30.

In the P-series, the larger the diameter of the end disk (D_e), the larger the pile end resistance. The R_p value of P-75 is 1.51 kN, and the bearing capacity factor (α) is 406 kN/m², which is 80% of the standard. In case of P-58, the end bearing capacity is $R_p=0.72$ kN ($\alpha=194$ kN/m²). It is about 1/2 of the P-75's and is almost the same as R_p of the closed end pile (CPT-20). The open end piles are used in the cement milk pile construction method because the cement milk should be filled up to the inner part of the piles. The piles with the end disk plate will exhibit sufficient end bearing capacities even if the stiffness of the root solidifying parts would be insufficient.

In the T-series, where the pile has an inner plate, TR-5 and TM-25 show almost the same results. The pile end resistances (R) of TR-5 and TM-25 are slightly larger than the result of the open end pile (OPT) due to the exiguous blockage effect. The inner plates have openings, and those areas are the same but the positions and shapes are different. However these differences have not affected the results because the clay on the root part moves with fluidity. The R_p values of R-5 and M-25 are 0.46 kN/m² and 0.45 kN/m² and about 25% of the standard pile (SP).

Bearing Capacity Factor and Aperture Ratio

Fig. 8 shows the relationship between the aperture ratio of the pile tip (r) and the bearing capacity factor (α). The α value is calculated by eq. 1, and A_p is the sectional area of the pile body. The aperture ratio r is the ratio of the opening area to the whole area of the pile tip. All test

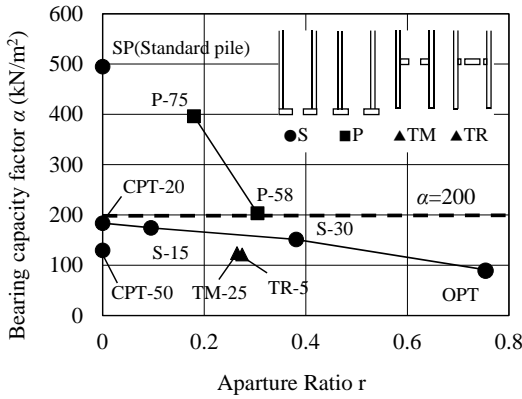


Fig. 8 Relationship between bearing capacity factor (α) and aperture ratio (r)

Table 3 Loading test results

Symbol	Aperture ratio (r)	$\delta/D=0.1$		$\delta/D=0.5D$	
		R_p (kN)	α (kN/m ²)	R_p (kN)	α (kN/m ²)
SP	0.00	1.84	495	4.03	1087
CPT-20	0.00	0.68	184	2.75	741
CPT-50	0.00	0.48	130	0.73	197
OPT	0.75	0.33	89	1.21	326
S-15	0.10	0.65	174	3.20	863
S-30	0.38	0.56	151	2.77	747
P-58	0.31	0.75	203	3.23	870
P-75	0.18	1.47	396	6.68	1801
TM-25	0.26	0.46	124	1.59	428
TR-5	0.27	0.45	122	1.46	394

results have a decreasing tendency proportional to the aperture ratio, that is, the larger aperture ratio (r), the smaller bearing capacity factor (α).

The α values of the S-series (including closed and open end piles) and T-series do not pass $\alpha>200$ kN/m², the standard of the prebored pile. However, only P-58 and P-75, both with an end disk plate, show larger values than the standard.

OBSERVATION TEST FOR BEHAVIOR OF PILE TIPS WITH FRAGILE ROOT PART

In order to observe the deformation process of the root part, an observation test was performed using a thin test tank which has transparent glass on one side. The actual stress and strain condition around the pile tip is a 3-dimensional axial symmetry state. Although the condition of this test is a 2-dimensional plane state, approximate behavior may be observed.

Test Object Preparation and Observation Method

The dimensions of the test tank are 800 mm in width, 650 mm in height, and 35 mm in inner thickness. A rectangular box made of aluminum is used as the test pile, and the dimensions are 50 mm in width x 75 mm in height x 30 mm in thickness. A steel rod, 12 mm in diameter, is attached to the test pile for vertical loading. In the same manner as the loading test, the exterior of the pile is covered by unhardened clay with a thickness is 20 mm.

After pushing the test tank over on its side, the test pile is placed. No. 5 silica sand in dry condition is used for the model ground, and the test ground is built up by the air-pluviation technique (see fig. 9). After fitting the glass on the top, the test tank is raised up. The test pile is pushed vertically with a speed of 1 mm/min, and photographs are taken every 1 mm of displacement.

Results of the Observation Test

Fig. 10 shows the deformation process of the root part of the pile. In the initial stage (0 - 10 mm), a small gap between the pile surface and the root part is generated, and a little displacement can be observed at the bottom of the root.

In the middle stage (10 - 30 mm), some cracks appeared from the corner of the bottom. The displacement of the bottom is growing, while a lateral displacement can be also observed.

In the final stage (30 - 40 mm), the cracks and displacements have grown, and the bottom of the root becomes thinner. Finally, breaking cracks reach the edge of the bottom, that is, the punching destruction has occurred.

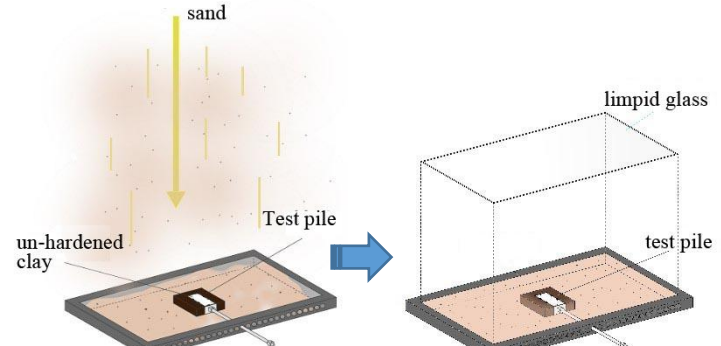


Fig. 9 Test object preparation

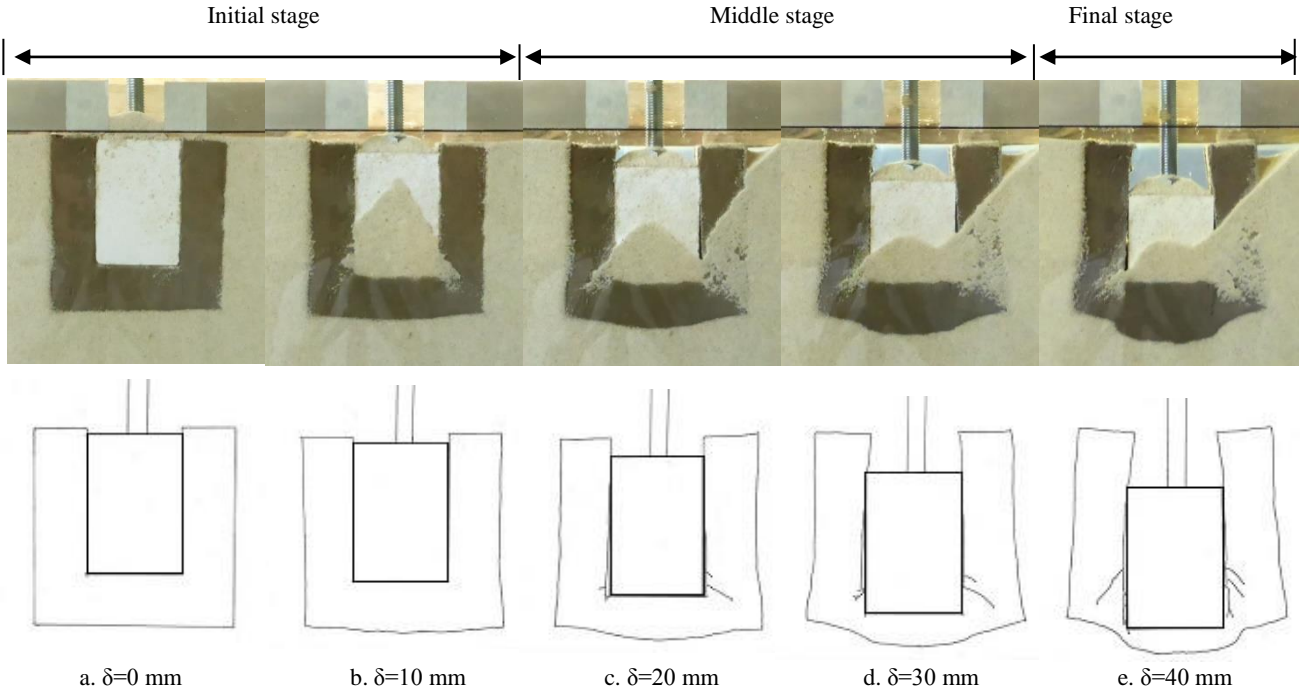


Fig. 10 Observation test result

The punching destruction will occur easily if the bottom of the root part is thin. However, if the root part is thicker, the end bearing resistance may not increase. Therefore, if the root part has not enough stiffness, and if the pile tip shape has a sufficient performance, a thinner bottom of the root might be better.

CONCLUSION

In the cement milk pile construction method, the end bearing capacity may be reduced due to the pile end openings and the fragile root part. Adding a large disk plate onto the pile end is one of the solutions of the problem. In this paper, we could examine the influence of the openings and of the insufficient stiffness of the root solidifying part. We could confirm the validity of the pile tip disk and of the thin bottom of the root.

ACKNOWLEDGEMENTS

Special thanks are due to Mr. K. Minagawa and Dr. Y. Kubo, System-Keisoku Co., Ltd., for their technical support. We would like to acknowledge Mr. Matsumoto and Mr. Harashima, students of Nihon University, for their cooperation in the laboratory experiment.

REFERENCES

- Goto, H, and Katsumi, T (1967). "Fundamental Studies on Settlements of Large Diameter Steel Pipe Piles", *Proc Japan Society of Civil Engineers, Japan society of civil engineers* (in Japanese), 138, 7-9.
 Katsumi, T, and Kitani, N (1982). "Fundamental Studies on The Effect of Blockade of Open Piles", *Proc of Japan Society of Civil Engineers, Japan society of civil engineers* (in Japanese), 323, 133-139.
 Kiya, Y, Kato, Y, Kuwabara, F (2007). "Model Tests on Vertical Bearing Performance of Enlarged Base of Buried Nodular Piles",



Photo 2 Preparation of model ground Photo 3 Observation condition

- Journal of Structural and Construction Engineering, Architectural Institute of Japan* (in Japanese), 615, 137-143.
 Miyazaki, S, Sato, H, and Kanuka, K (2014). "Fundamental Study on Vertical Pile-end Bearing Capacity of Pile -Model Experiments for Closed End Pile and Open End Pile Using Bored Precast Pile Construction Method-", *Proc 11th Kanto Branch of The Japanese Geotechnical Society* (in Japanese), CD-ROM.
 Miyazaki, S, Sato, H, Kanuka, K, Harigaya, Y (2015). "Consideration for End Shape of a Pile for Prebored Pile Construction Method", *Proc 25th International Offshore and Polar Engineering Conference (ISOPE)*, 780-784.
 Ueno, K, Kurachi, S, Ohi, A and Yokoyama, Y (1993). "Shape Effect on Failure Mechanism of Tip Protected Pile", *Proc 28th Japan National Conference on Geotechnical Engineering* (in Japanese), E-4, 1731-1734.